

## Polymer $\theta$ -point as a knot delocalization transition

E. Orlandini,<sup>1</sup> A. L. Stella,<sup>1,2</sup> and C. Vanderzande<sup>3,4</sup><sup>1</sup>*INFN-Dipartimento di Fisica, Università di Padova, I-35131 Padova, Italy*<sup>2</sup>*Sezione INFN, Università di Padova, I-35131 Padova, Italy*<sup>3</sup>*Departement WNI, Limburgs Universitair Centrum, Universitaire Campus, 3590 Diepenbeek, Belgium*<sup>4</sup>*Instituut voor Theoretische Fysica, Katholieke Universiteit Leuven, Celestijnenlaan 200D, 3001 Heverlee, Belgium*

(Received 13 November 2002; published 19 September 2003)

We study numerically the tightness of prime flat knots in a model of self-attracting polymers with excluded volume. We find that these knots are localized in the high temperature swollen regime, but become delocalized in the low temperature globular phase. Precisely at the collapse transition, the knots are weakly localized. Some of our results can be interpreted in terms of the theory of polymer networks, which allows one to conjecture exact exponents for the knot length probability distributions.

DOI: 10.1103/PhysRevE.68.031804

PACS number(s): 36.20.Ey, 02.10.Kn, 64.60.Ak, 87.15.Aa

The presence of knots in single-ring macromolecules, or of chain entanglement in polymer melts, has fundamental consequences at the physical, chemical, and biological level. For example, the dynamics of a ring polymer in a gel depends crucially on its topology [1]. The replication and the transcription of circular DNA are controlled by enzymes affecting the topology, the topoisomerases [2]. Knots have even been identified in some proteins in their native state [3]. It is easy to imagine the importance that the degree of localization of knots can have. In the folding of a protein it must make quite a difference whether the knot is tight and localized within a restricted region of the backbone or not. A loose knot poses less restrictions to the exploration of configuration space in the search for the native state. Similarly, one could expect that the degree of knot localization can strongly influence the function of topoisomerases.

These examples all concern heteropolymers in nonequilibrium situations. Here we investigate the interplay between topology and temperature in a simpler context by studying the *equilibrium* properties of (prime) knots in *homopolymers* when these are cooled below their  $\theta$  temperature. Under such conditions we find that knots definitely lose their usual property of being localized within restricted portions of the chains.

It is very difficult to include topological constraints within a statistical mechanical description of a polymer, since they imply a global control of its conformations [4]. So far, most works have concentrated on the probability of occurrence of knots [5] and much less has been done on the physically relevant problem of precisely quantifying the knot size. Besides attempts to measure knot size directly [6], most studies have given only indirect and often incomplete information on knot localization. For a ring polymer with excluded volume it was found numerically that the presence of a prime knot leads to a simple multiplication of the partition sum with a factor proportional to the length  $L$  of the macromolecule [7]. Moreover, for the relation between the radius of gyration and  $L$  [Eq.(1)], evidence was given that neither the amplitude  $A$  [8] nor the critical exponent  $\nu$  depends on the topology [8,9]. These results suggest that knots are somehow localized within small portions of the chain. Unfortunately, the length of such portions, to be considered as the size of

the knots, is difficult to define and to measure. However, under suitable conditions this is not true for knots in ring polymers that are fully adsorbed on a plane [10]. The configurations of such rings would be similar to the planar projections on which the knot theory bases the determination of topological invariants [11], and are called flat knots. If adsorption is induced by a very strong short-range or contact potential, overlaps of the polymer with itself are strongly disfavored energetically, so that the equilibrium configurations always show the minimum number of crossings compatible with the knot topology. Below we always assume such a strong adsorption. So, for example, in the case of a trefoil knot ( $3_1$ ), each configuration will consist of three overlap crossings suitably connected by six arcs. In Ref. [12] it was shown that for a ring of length  $L$  with only excluded volume there is typically one of the arcs whose length is of order  $L$ , whereas the total length of all the other arcs,  $l$ , which can be considered as the size of the knot, is much smaller:  $l \ll L$ . More precisely,  $\langle l \rangle$ , the average value of  $l$ , was found not to diverge with  $L$ . In this case one says that the knot is localized. If in contrast,  $\langle l \rangle \sim L^t$ , one speaks of weak localization ( $0 < t < 1$ ) or delocalization ( $t = 1$ ) of the knot.

In the present paper, we investigate the size of flat knots of polymers with excluded volume and attractive self-interactions as a function of temperature  $T$ . Under these circumstances the polymer will undergo a collapse transition from a coil to a globule shape below a  $\theta$ -point temperature  $T_\theta$  [13]. Our main result is that in the collapsed phase knots are delocalised. At the  $\theta$  point, we find them to be weakly localized with  $t = 3/7$ .

A model for flat knots can be defined [14] on the square lattice whose set of edges is extended with the diagonals of the squares. The bonds of the polymer can visit each edge and each vertex of this extended lattice at most once. A diagonal can only be occupied if at the same time the other, perpendicular diagonal within the same elementary square is also occupied. Each pair of occupied diagonals represents a crossing (not to be considered as a lattice vertex) in the projection of the knot. Thus, one has to further specify which of the two diagonal bonds goes under the other one. The model is simulated within the grand canonical ensemble, where a

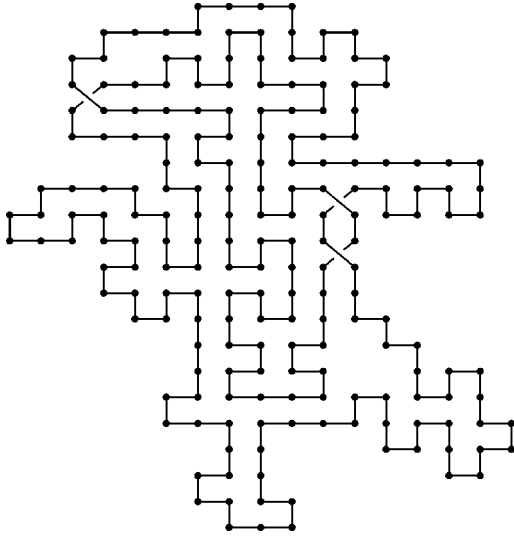


FIG. 1. Typical configuration of a polymer with a trefoil knot in the low  $T$  collapsed phase.

fugacity  $K$  is assigned to each bond of the ring polymer, while the number of crossings is constrained to the minimum consistent with the topology. As usual, to induce  $\theta$  collapse, we associate an attractive energy with each pair of lattice vertices that is visited by nonconsecutive bonds. Fig. 1 shows a configuration with the topology of a trefoil.

In our Monte Carlo approach, a Markov process in the configuration space of the polymer is constructed by a combination of local and nonlocal moves. These are chosen as in Ref. [14] and are such as to ensure invariance of the polymer topology. Averages at fixed  $T$  are then calculated using a multiple Markov chain (MMC) implementation in the fugacity  $K$  [15]. This guarantees an exhaustive sampling of configurations also at rather low temperatures [16]. First, we obtain precise estimates of  $K_c(T)$ , the critical fugacity above which the grand canonical average  $\langle L \rangle = \infty$ . Since for the case of a flat trefoil, there are always only three pairs of diagonals occupied, we can expect that  $T_\theta$  is very close to the value of an interacting self-avoiding ring model without crossings. To verify this, we investigated the average squared radius of gyration  $\langle R_g^2 \rangle_L$  [17] as a function of  $L$  for this case. Figure 2 reports our results for different  $T$ 's. One expects that asymptotically

$$\langle R_g^2 \rangle_L \sim AL^{2\nu}. \quad (1)$$

Our data clearly show the expected three regimes. At high  $T$ 's, we are in a self-avoiding walk regime with  $\nu \approx 3/4$ . At low  $T$ 's we determine an exponent  $\nu = 0.49 \pm .02$ , consistent with the value appropriate for a collapsed polymer,  $\nu = 1/2$ . Finally, close to  $1/T = 0.67$  we find a  $\nu$  in agreement with that at the  $\theta$  point, i.e.,  $\nu = 4/7$  [18]. Hence, we estimate  $1/T_\theta = 0.67 \pm .02$ , fully consistent with determinations for unknotted rings [19]. We also conclude that the exponent  $\nu$  at the  $\theta$  point and in the collapsed phase is not modified by changing the topology from that of a flat unknot to that of a flat trefoil.

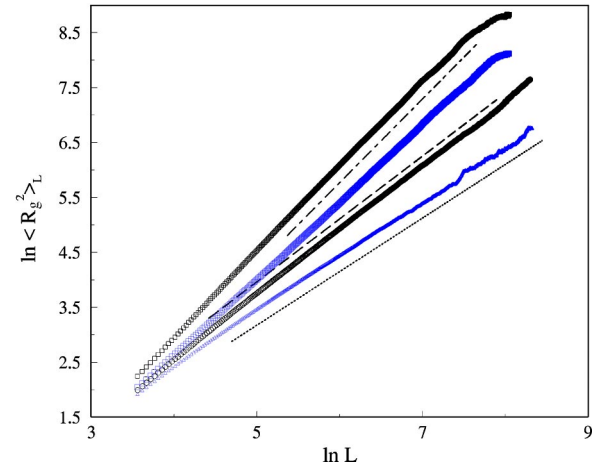


FIG. 2. Log-log plot of  $\langle R_g^2 \rangle_L$  as a function of  $L$  for a ring with trefoil knot. From top to bottom:  $1/T = 0, 0.50, 0.67 (\approx 1/T_\theta), 0.8$ . The dot-dashed, the dashed, and the dotted lines have slopes  $3/2$ ,  $8/7$ , and  $1.0$ , respectively.

In order to characterize the tightness of the trefoil knot, we consider all its six arcs and determine the statistics of their lengths  $l_1 \leq l_2 \leq \dots \leq l_6$ . Clearly the largest arc must always have a length proportional to  $L$ . In Fig. 3, we plot the average length of the second largest arc, i.e.,  $\langle l_5 \rangle_L$ , as a function of  $L$ . For high  $T$ 's, we see that  $\langle l_5 \rangle_L$  saturates at large enough  $L$ . Moreover, all the other arc lengths remain much smaller, typically only a few bonds. We conclude that in the swollen regime the knot is localized. The quantity  $\langle l \rangle_L / L = \langle (\sum_{i=1}^5 l_i) \rangle_L / L$  approaches zero when  $L \rightarrow \infty$ .

At  $T_\theta$ , we find instead that  $\langle l_5 \rangle_L$  grows as  $L^t$ , with  $t = 0.44 \pm 0.02$ . All other lengths remain again very small. Thus, the typical shape of the polymer appears to be that of a figure eight, as found also with excluded volume only [12]. We thus conclude that the knot is weakly localized at the  $\theta$  point.

Finally, and most interestingly, we find that in the col-

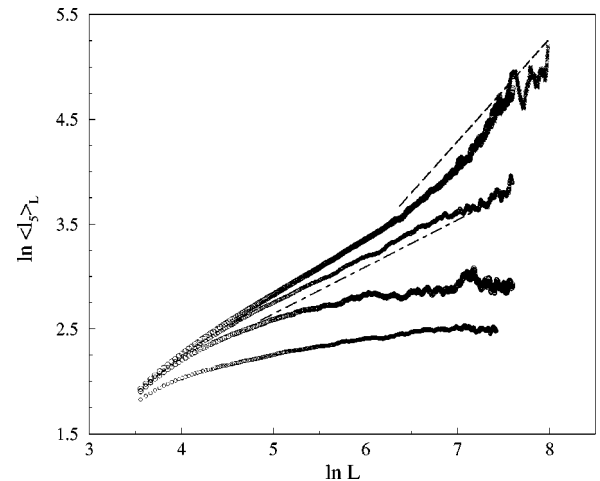


FIG. 3. Log-log plot of  $\langle l_5 \rangle_L$  as a function of  $L$  for a trefoil knotted polymer. From bottom to top:  $1/T = 0, 0.50, 0.67, 0.8$ . The dot-dashed line has a slope  $0.44$  whereas the dashed line has slope  $1.0$ .

lapsed phase, and for  $L$  values that are sufficiently large,  $\langle l_5 \rangle_L \sim L$ , implying a *delocalization* of the knot. In this case, there is ample evidence that also the average length of smaller arcs, such as  $\langle l_4 \rangle_L$ , starts to grow proportional to  $L$  for still longer polymer lengths. We suspect that in sufficiently long polymers all average arc lengths will become extensive in  $L$ . Thus, a description in terms of a figure eight breaks down in the collapsed phase.

It is possible to associate a polymer network  $\mathcal{G}$  with  $N$  segments [20] to each flat knot configuration with the same number of nonmicroscopic arc lengths [12]. Interest in polymer networks was revived recently by a successful development concerning DNA denaturation [21]. The same type of approach was subsequently applied in Ref. [12] where it was found that flat knots with excluded volume are always localized. Our data for  $T > T_\theta$  support this conclusion, and moreover convincingly show that localization is present throughout the whole high temperature phase (Fig. 3).

On the basis of a network description, this time with *interacting* polymer segments, it is possible to gain further insight into some of our results. Let  $\mathcal{G}$  be such a network with  $n_k$  vertices of degree  $k$  connected by  $N$  arcs of total length  $L$ . The partition sum  $Z_{\mathcal{G}}(l_1, \dots, l_N)$  of the network scales as [20,22]

$$Z_{\mathcal{G}}(l_1, \dots, l_N) = K_c^{-L} l_N^{\gamma_{\mathcal{G}}-1} F_{\mathcal{G}}\left(\frac{l_1}{l_N}, \dots, \frac{l_{N-1}}{l_N}\right), \quad (2)$$

where  $F_{\mathcal{G}}$  is a scaling function and  $\gamma_{\mathcal{G}} = 1 - \nu d \mathcal{L} + \sum_k n_k \sigma_k$ . Here  $d$  is the dimension of space and  $\mathcal{L}$  is the number of independent loops in the network. The lengths of the network segments, corresponding to macroscopic knot arcs, are  $l_1 \leq \dots \leq l_N$ . Finally, the exponents  $\sigma_k$  are anomalous dimensions associated to the  $k$ -leg vertices of the field theory describing the polymer in the continuum limit [20]. In two dimensions, Coulomb gas methods allow an exact determination of the  $\sigma_k$ 's. In particular, at  $T = \infty$ , where polymers are described by the  $n \rightarrow 0$  limit of a critical  $O(n)$  model, one has  $\sigma_k = (2-k)(9k+2)/64$  [20]. On the other hand, the  $\theta$  point is described by the critical low temperature phase of the  $O(n=1)$  model, for which  $\sigma_k = (2-k)(2k+1)/42$  [18]. Finally, following Ref. [23], we assume that the properties of the low  $T$  regime can be related to those of dense polymers, which are described by the low  $T$  phase of the  $O(n=0)$ -model. For this case special care has to be taken, and one ends up with a scaling form for  $Z_{\mathcal{G}}$ , which is slightly different from Eq.(2) [24]. Yet, despite these differences, the network picture can still be applied to flat knots with  $\sigma_k = (4-k^2)/32$  [24].

When in a network one or more arcs become very short, and hence the crossings on which they are incident approach each other very closely, the network should be replaced by another contracted one with fewer segments and crossings, and a different  $\gamma_{\mathcal{G}}$ . In this way, it can be understood that even though any projection of a trefoil contains six arcs, at a more coarse grained level, the typical contribution appearing in a numerical simulation can come from a network with fewer crossings. This is what happens, for example, at the  $\theta$  point, where we found that the flat trefoil looks like a figure

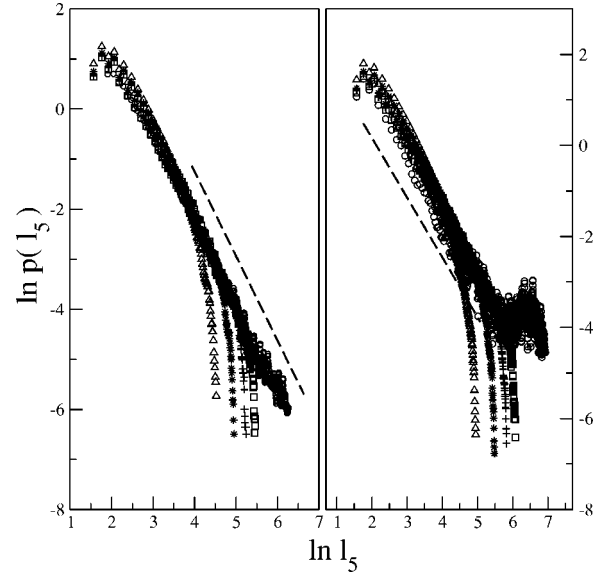


FIG. 4. Log-log plot of  $p(l_5)$ . On the left (right), we show our data at  $1/T_\theta \approx 0.67$  ( $1/T = 0.8$ ). The dashed lines have slopes of  $-1.63$  and  $-1.34$ . Different symbols refer to different canonical averages with  $L = 200$  ( $\Delta$ ),  $L = 400$  ( $*$ ),  $L = 600$  ( $+$ ),  $L = 800$  ( $\square$ ), and  $L = 1400$  ( $\circ$ ).

eight [ $l_4 \sim O(1)$ ]. At  $T_\theta$ , where  $\nu = 4/7$ , Eq. (2) predicts that the partition function of a figure eight network scales as

$$Z_8 = K_c^{-L} (L-l)^{\gamma_8-1} F_8\left(\frac{l}{L-l}\right), \quad (3)$$

with  $\gamma_8 = -12/7$ . For  $l/L \rightarrow 0$ , this partition sum should in its turn reduce to that of a self-avoiding ring at the  $\theta$  point, which is known to scale as  $Z \sim K_c^{-L} L^{-\nu d}$ . This simple analysis [21] then teaches us that  $F_8(x) \sim x^{-c}$  for  $x \rightarrow 0$ , with  $c = -(\gamma_8 - 1 + \nu d) = 11/7 \approx 1.57$ . Hence, for  $l \ll L$  we predict that

$$Z_8 \sim K_c^{-L} (L-l)^{-\nu d} l^{-c}. \quad (4)$$

In Fig. 4 (left) we present our data for  $p(l_5)$ , the probability distribution of  $l_5$ , at  $T = T_\theta$ . From Eq. (4) it follows that  $p(l_5) \sim l_5^{-c}$ . A fit to this form leads to  $c = 1.63 \pm 0.08$ , consistent with the above prediction. Finally, we get from Eq. (4) that  $\langle l_5 \rangle_L \sim L^{3/7}$ , in good agreement with the numerical estimate  $\langle l_5 \rangle_L \sim L^{0.44 \pm 0.02}$ . We expect that  $t = 3/7$  is an exact result which characterizes the weak localization of the knot at the  $\theta$  point.

At  $T < T_\theta$ , an analysis using the results of Ref. [24] can still be made for a ring with the shape of a figure eight, and leads to the prediction  $c = 11/8$ . In Fig. 4 (right), we also show our data for  $p(l_5)$  at  $1/T = 0.8 > 1/T_\theta$ . There is indeed an initial power law decay with an exponent  $1.34 \pm 0.12$ . But in this case,  $p(l_5)$  flattens for larger  $l_5$  values and it is this broadening which eventually leads to the delocalization of the knot. The preasymptotic slope indicates that for relatively small  $l_5$ , the weakly localized figure eight network configurations are still dominating the partition sum. When  $\langle l_5 \rangle_L \sim L$  one can get no help from network scaling arguments in

determining  $p(l_5)$ . Indeed, such arguments are only valid for  $l_5 \ll L$  which is not the relevant range when  $\langle l_5 \rangle_L \sim L$ .

We verified that also for other prime knots, such as the  $5_1$  and  $7_1$  [11], the typical network configuration at  $T=T_\theta$  is still the figure eight and delocalization occurs for  $T < T_\theta$ .

When in our model the number of crossings is not restricted to be minimal, characterizing the flat knot size becomes as difficult as for the three-dimensional case. For a given configuration, one could then define  $l$  as the minimal length of an open portion of the ring within which a knot of the same type as that of the whole chain can still be detected (see Ref. [6]). The presence of many crossings could weaken

localization or enhance delocalization with reference to such more general definition of  $l$ . Indeed, preliminary applications of such computationally more expensive criteria directly to polygons with excluded volume in three dimensions show that knots are localized, but only weakly [25]. This is also indicated by studies relating the knot size to the response to applied forces [26]. The localization prevailing in the excluded volume controlled regime in three dimensions suggests that the delocalization transition found here could also hold with unrestricted crossings, and, even more important, for the three-dimensional case.

Financial support from INFN-PAIS 01 and MIUR-COFIN 01 is acknowledged.

- 
- [1] S.A. Wasserman and N.R. Cozzarelli, *Science* **232**, 951 (1986); S.P. Obukhov, M. Rubinstein, and T. Duke, *Phys. Rev. Lett.* **73**, 1263 (1994).
- [2] B. Alberts *et al.*, *Molecular Biology of the Cell* (Garland Science, New York, 2002).
- [3] F. Takusagawa and K. Kamitori, *J. Am. Chem. Soc.* **118**, 8945 (1996); W.R. Taylor, *Nature (London)* **406**, 916 (2000).
- [4] A.L. Kholodenko and T.A. Vilgis, *Phys. Rep.* **298**, 254 (1998); A.Yu. Grosberg, *Phys. Rev. Lett.* **85**, 3858 (2000).
- [5] J.P.J. Michels and F.W. Wiegel, *Phys. Lett. A* **90**, 381 (1982); D.W. Sumners and S.G. Whittington, *J. Phys. A* **21**, 1689 (1988); E.J. Janse van Rensburg and S.G. Whittington, *ibid.* **23**, 3573 (1990); K. Koniaris and M. Muthukumar, *Phys. Rev. Lett.* **66**, 2211 (1991); T. Deguchi and K. Tsurusaki, *Phys. Rev. E* **55**, 6245 (1997).
- [6] V. Katritch, W.K. Olson, A. Vologodskii, J. Dubochet, and A. Stasiak, *Phys. Rev. E* **61**, 5545 (2000).
- [7] E. Orlandini, M.C. Tesi, E.J. Janse van Rensburg, and S.G. Whittington, *J. Phys. A* **29**, L299 (1996).
- [8] E. Orlandini, M.C. Tesi, E.J. Janse van Rensburg, and S.G. Whittington, *J. Phys. A* **31**, 5953 (1998).
- [9] S.R. Quake, *Phys. Rev. Lett.* **73**, 3317 (1994).
- [10] Examples range from DNA: B. Maier and J.O. Rädler, *Phys. Rev. Lett.* **82**, 1911 (1999), to vibrated granular chains: E. Ben-Naim, Z.A. Daya, P. Vorobieff, and R.E. Ecke, *ibid.* **86**, 1414 (2001); M.B. Hastings, Z.A. Daya, E. Ben-Naim, and R.E. Ecke, *Phys. Rev. E* **66**, 025102 (2002). The latter are slightly but definitely out of equilibrium.
- [11] K. Murasugi, *Knot Theory and its Applications* (Birkhäuser, Boston, 1996).
- [12] R. Metzler, A. Hanke, P.G. Dommersnes, Y. Kantor, and M. Kardar, *Phys. Rev. Lett.* **88**, 188101 (2002).
- [13] C. Vanderzande, *Lattice Models of Polymers* (Cambridge University Press, Cambridge, 1998).
- [14] E. Guitter and E. Orlandini, *J. Phys. A* **32**, 1359 (1999).
- [15] M.C. Tesi, E.J. Janse van Rensburg, E. Orlandini, and S.G. Whittington, *J. Stat. Phys.* **82**, 155 (1996).
- [16] Our MMC are based on ten different  $K$  values. For each one we sample  $2 \times 10^5$  independent configurations, corresponding to  $\sim 10^{11}$  local moves.
- [17]  $\langle \dots \rangle_L$  is a canonical average over a subset of rings with length  $\approx L$ .
- [18] B. Duplantier and H. Saleur, *Phys. Rev. Lett.* **59**, 539 (1987).
- [19] F. Seno and A.L. Stella, *J. Phys. (France)* **49**, 739 (1988); G.T. Barkema, U. Bastolla, and P. Grassberger, *J. Stat. Phys.* **90**, 1311 (1998).
- [20] B. Duplantier, *J. Stat. Phys.* **54**, 581 (1989).
- [21] Y. Kafri, D. Mukamel, and L. Peliti, *Phys. Rev. Lett.* **85**, 4988 (2000).
- [22] L. Schäfer, C. Von Ferber, U. Lehr, and B. Duplantier, *Nucl. Phys. B* **374**, 473 (1992).
- [23] B. Duplantier, *Phys. Rev. Lett.* **71**, 4274 (1993).
- [24] B. Duplantier and H. Saleur, *Nucl. Phys. B* **290**, 291 (1987).
- [25] B. Marcone, E. Orlandini, and A. L. Stella (unpublished).
- [26] O. Farago, Y. Kantor, and M. Kardar, *Europhys. Lett.* **60**, 53 (2002).